Mitigation of the effects of multivalent ion transport in reverse electrodialysis

J. Moreno[a,b], V. Díez[a], M. Saakes[a], K. Nijmeijer[b,*]

[a] *Wetsus, European Centre of Excellence for Sustainable Water Technology, Oostergoweg 9, 8911MA Leeuwarden, The Netherlands*
[b] *Membrane Science & Technology, University of Twente, P.O. Box 217, 7500AE Enschede, The Netherlands*

ARTICLE INFO

ABSTRACT

Reverse electrodialysis (RED) is a sustainable method to harvest energy using the salinity gradient between fresh and seawater. RED technology is developing but efficiencies are still limited when using natural feed water sources. One significant constraint is induced by the presence of multivalent ions in sea and river water (i.e. Mg^{2+}, Ca^{2+}, SO_4^{2-}). Uphill transport and an increase in membrane resistance in the presence of magnesium ions significantly reduce the power density output obtainable. The choice of cation exchange membrane determines the magnesium transport and as such the power density. Here we investigate four cation exchange membrane types and relate their properties to the stack performance using three different magnesium concentrations on either river and/or seawater side: 1) a highly cross-linked styrene-divinyl benzene monovalent selective cation exchange membrane (Neosepta CMS); 2) a monovalent selective cation exchange membrane that contains a thin polyethyleneimine (PEI) anion exchange layer (Selemion CSO); 3) a multivalent ion (e.g. magnesium) permeable cation exchange membrane with an engineered molecularly open structure facilitating the transport of multivalent ions as recently developed (T1 Fujifilm); 4) a standard cation exchange membrane (Type I Fujifilm (reference)). The first two membranes both retain magnesium ions, while the other two membranes are considered permeable for magnesium ions.

The results show that power density strongly depends on the composition of both river and seawater. Power density decreases in the presence of magnesium, an effect being strongest with magnesium at both river and seawater side, followed by the river water side and the seawater side. The negative effect of multivalent ion transport against the concentration gradient, so called uphill transport, in RED can be significantly minimized when monovalent selective membranes such as the highly cross-linked Neosepta CMS membrane or the AEM coated Selemion CSO membrane are used. However, the use of such membranes directly results in a strong increase in membrane resistance due to the lower ion mobility of magnesium ions inside these membranes. As a consequence, power densities in RED are not improved. Especially at high magnesium concentrations, this effect is very strong at higher concentrations, the membranes are no longer able to retain magnesium ions effectively.

More beneficial is the application of multivalent permeable membranes with a more 'open' structure that allow the free movement of both sodium and magnesium ions through the membrane. Maybe somewhat counter intuitively, such membranes (especially the Fujifilm multivalent permeable T1 membrane) have low resistance values combined with reasonable OCV values leading to high power densities under almost all magnesium concentrations, especially at long term applications. Highest power densities well exceeding 0.3 W/m^2 are still obtained when only sodium is present. However, when magnesium ions are present power densities in the order of 0.2–0.25 W/m^2 can still be obtained for these membranes.

1. Introduction

Reverse electrodialysis (RED) is a sustainable method to harvest energy using the salinity gradient between fresh and sea water [1–3]. Ion exchange membranes (IEMs) separate the concentrated salt solution (sea water) from the diluted salt solution (river water) in RED. Anion

exchange membranes (AEMs) are alternated with cation exchange membranes (CEMs) and river and seawater flow alternatively on either side of the membranes. The chemical potential difference created across the membranes is the driving force for this process: ions permeate through the membranes in accordance with their charge. At the electrodes, the ionic current is converted into an electrical current through

redox reactions generating electricity when closing the external electric circuit. Ion exchange membranes are non-porous dense structures, composed of a polymer matrix containing ionic groups, either negatively charged (CEMs) or positively charged (AEMs). Ion exchange membranes transport ions with the opposite charge as the membrane charge, the so-called counter ion transport. So cation exchange membranes are negatively charged and transport cations (e.g. Na^+, Mg^{2+}, Ca^{2+}), while anion exchange membranes are positively charged and transport anions (e.g. Cl^-, SO_4^{2-}). CEMs normally contain sulfonic or carboxylic acid groups, whereas AEMs contain quaternary amine groups. As the membranes are never 100% selective, also limited transport of ions with the same charge as the membrane occurs, the so-called co-ion transport. The ratio of the amount of charge transported by the counter-ions and by the co-ions is called the membrane permselectivity.

RED technology is developing but energy efficiencies are still limited when using natural feed water sources [4]. One significant constraint is due to the presence of multivalent ions in sea and river water (i.e. Mg^{2+}, Ca^{2+}, SO_4^{2-}). The presence of these multivalent ions in river water causes uphill ion transport in IEMs [5,6]. Uphill transport refers to the process of ion transport in the direction opposite to the concentration gradient, i.e. from low to high concentration (Fig. 1).

In uphill transport, counter-ions are transported in both directions until the electromotive forces of the ionic species are balanced (equilibrium) and a net flux of electrical charges no longer exists. Donnan dialysis uses uphill ion transport phenomena as driving force of the process [7]. In the system under study, using artificial river and sea water, 2 Na^+ ions (downhill transport in the direction of the concentration gradient) are exchanged by 1 Mg^{2+} or 1 Ca^{2+} ion (uphill transport opposite the direction of the concentration gradient). In RED, uphill transport leads to significant energy efficiency losses. Vermaas et al. [6] reported a loss in power density up to 50% at laboratory scale using standard membranes and synthetic feed waters containing 10% $MgSO_4$ in a RED stack. This power density loss was basically attributed to a loss in OCV and barely to an increase in electrical resistance of the membrane. Post et al. [5] studied the RED stack voltage response, the electrical resistance and the effluent ionic concentration when multivalent ions are present. Post et al. [5] concluded that monovalent ion selective membranes could be a good alternative for reverse electrodialysis and particularly if high multivalent ion concentrations are present in the diluted side. However, the improvement on power density might not be as high as expected, due to a loss in monovalent permselectivity and increase on stack resistance in time.

Uphill ion transport causes a reduction in the stack voltage, but also an increase in membrane electrical resistance due to lower diffusion coefficients of Mg^{2+} and SO_4^{2-} compared to Na^+ and Cl^-. Also multivalent ions get bonded to ion exchange groups inside the membrane.
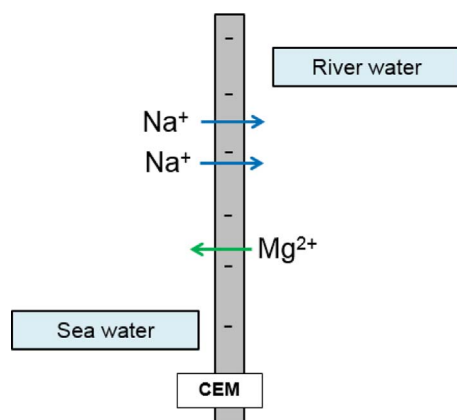

Fig. 1. Uphill transport of one multivalent Mg^{2+} ion to replace two monovalent Na^+ ions in a cation exchange membrane.

Therefore, a significant decrease in the obtained power density is observed [8]. The influence of multivalent ions on IEMs has been reported to be more significant in CEMs than in AEMs due to the larger voltage drop [6].

Recently the research on membrane development to minimize the effect of multivalent ions in RED by modifying ion selective membranes has intensified. For instance Güler et al. [9] increased the monovalent ion selectivity through the formation of a highly cross-linked CEM layer on top of an AEM by photo-polymerization (UV). Monovalent ion selectivity was improved by implementing a CEM layer on the top of an AEM, in order to increase the electrostatic repulsion between multivalent ions and membrane surface charge. Higher gross power density was not obtained, however, an improvement on antifouling properties was achieved. Rijnaarts et al. [10] presented a new strategy to overcome the unwanted effects of multivalent ions in RED, by ordering the CEM negative charged groups and providing pathways for ion transport. This so-called multivalent ion permeable membrane has a low membrane electrical resistance and binding of multivalent ions to the charged groups of the membrane was reduced [11]. As a continuation of this research, we here investigate and compare systematically three different membrane strategies to mitigate the effect of multivalent ions in RED (Fig. 2).

The first strategy relies on the use of a highly cross-linked CEM that blocks the transport of multivalent ions and allows the transport of monovalent ions only. Such a membrane acts as an ion sieve when differences in hydrated ionic radii are present [6]. The effective membrane pore size (i.e. membrane ion pathaway) decreases with increasing cross-linker agent concentration (i.e. phenol, divinylbenzene) and so the permeation of multivalent ions decreases. This increase in cross-links increases the permselectivity for monovalent ions over multivalent ions. However, electrical resistance and concentration polarization increase with the content of cross-linker.

The second strategy relies on the application of an oppositely charged top layer on the membrane surface (i.e. a layer with a charge opposite to the membrane charge). Sata et al. [12,13] investigated this strategy by forming a cationic charged layer on the CEM surface to increase the electrostatic repulsion of multivalent ions. A layer of polyethyleneimine (PEI) was formed by acid-amide bonding or adsorption (ion exchange or monolayer adsorption) and creates multivalent ion rejection due to the higher charge density of the multivalent ions. The third, novel strategy, is a multivalent ion permeable membrane i.e. no rejection towards multivalent ions but facilitation of multivalent transport. This approach has only recently been developed especially for application in RED [10]. Till now, almost all IEM membranes used in RED were designed or optimized for other applications (such as desalination or electrodialysis (salt production or acid recovery)). The multivalent ion permeable membrane is an IEM intentionally designed to overcome the challenges of using real feed waters in RED. For this purpose, the membrane is designed such that multivalent ion transport across the membrane is facilitated by fabricating a membrane with a more open structure not increasing the electrical membrane resistance when multivalent ions are transported.

The effect of these three approaches on open circuit voltage, stack resistance and RED power density are investigated. All data are compared to the reference case using a standard CEM. Also, to provide insight in the mass transport mechanisms and consequences of the presence of multivalent ions, measurements were performed with NaCl solutions only on both river and seawater side, 1) with $MgCl_2$ on both sides; 2) with $MgCl_2$ on the river water side and NaCl on the sea water side and 3) with $MgCl_2$ on the seawater side and NaCl on the river water side. $MgCl_2$ concentrations of 10%, 25% and 50% were used in all cases. Additionally, for the 25% $MgCl_2$ case the mass transfer of sodium ions and magnesium ions is monitored in time to unravel the ion transport directions.

Highly cross-linked   **Thin AEM coated layer**   **Multivalent ion permeable**
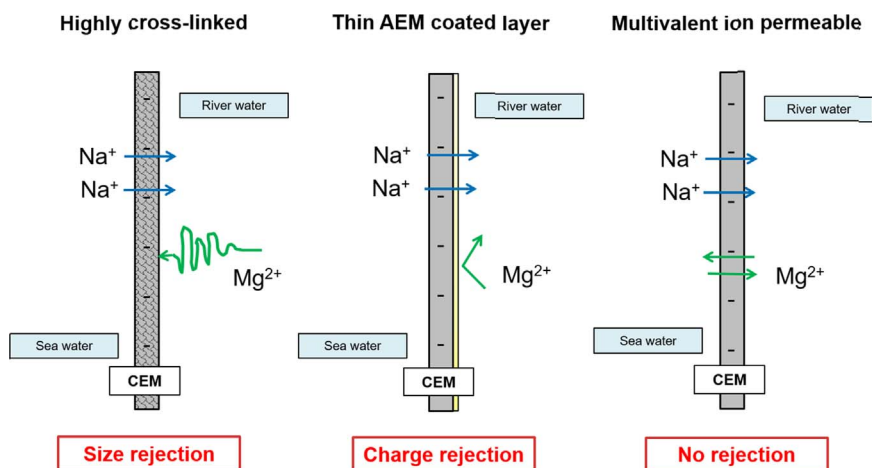

Fig. 2. Illustration of different membrane strategies to mitigate the effect of multivalent ions in RED. (For interpretation of the references to color in this figure legend, the reader is referred to the web version of this article.)

2. Materials and methods

2.1. Stack configuration

Four similar RED stacks (REDstack BV, the Netherlands) each equipped with a different CEM type (depending on the strategy) were evaluated. Each stack contained the specific targeted CEM, while the AEM was the same in all cases. The following CEMs were evaluated (each in a different stack): I) T1 (multivalent ion permeable membrane, Fujifilm BV); II) CMS (highly cross-linked membrane, Neosepta); III) CSO (thin AEM one-side-coated membrane, Selemion) and IV) Type I (standard-grade CEM membrane (as the reference case), Fujifilm BV). In all cases, a Fujifilm AEM Type I membrane was used as anion exchange membrane and a Neosepta CMX was used as shielding membrane at the final ends of the stack next to the electrodes. The specifications of the membranes are listed in Table 1.

Each stack was composed of 5 AEMs, 4 of the investigated CEMs and 2 additional shielding CEMs to close the membrane pile at the sides and keep the electrolyte solution in the electrolyte compartment. The length and width of the membrane compartments is 10 × 10 cm, yielding a total membrane area per stack of 0.1 m². Woven spacers of 485 μm (Sefar 06–700/53, Switzerland) were introduced between the membranes to accommodate the feed waters. Silicone rubber gaskets were also placed between the closing membranes and the end plates to seal the electrolyte compartment. Titanium electrodes (mesh 1.7 m²/m², area 96.04 cm²) with a mixed ruthenium/iridium metal oxide coating (Magneto Special Anodes BV, The Netherlands) were used as anode and cathode and connected to a potentiostat (Ivium Technologies, The Netherlands). A solution of 0.05 M $K_3Fe(CN)_6$, 0.05 M $K_4Fe(CN)_6$ and 0.25 M NaCl in demineralized water was used as electrolyte solution and recirculated through the electrolyte compartments by an adjustable peristaltic pump (Cole-Parmer, Masterflex L/S Digital drive, USA) at a flow rate of 150 ml/min. The electrolyte was kept under a slight overpressure of 0.5 bar to avoid bulging of the feedwater compartments.

2.2. Feed water

Artificial river water and seawater were used during the experiments. Solutions were composed of a mixture of dissolved NaCl (99.5% purity, ESCO, The Netherlands) and $MgCl_2$ (BDH, Prolabo©, Belgium). The total salt concentration of the artificial seawater was 0.508 M and that of the river water was 0.017 M. When considering mixtures of NaCl and $MgCl_2$, a molar percentage of 10%, 25% and 50% of the total dissolved salt was accounted for by $MgCl_2$ and the remaining amount of dissolved salt was NaCl in order to maintain the molarity of the feed waters. The experiment was performed at 23.0 ± 0.5 °C. Both temperature and conductivity were checked at the beginning of each experiment. The flow velocity of the feed water was 1 cm/s in all cases, which is equivalent to a flow of 145 ml/min. The effluent was not reused, i.e. fresh feed water was supplied continuously.

2.3. Experimental design

A fixed sequence of inflowing feed waters was followed (Table 2) in order to create three different scenarios (I) $MgCl_2$ at both sides; ii) $MgCl_2$ at the river water side only; III) $MgCl_2$ at the seawater side only.

The molar percentage of $MgCl_2$ was varied from 10%, 25% to 50%. In between the three different scenarios a 100% molar NaCl solution was fed to the compartments during 1 h. Experiments were done in duplicate and some in triplicate. Effluent sampling was performed on the experiments with 25% $MgCl_2$ solutions in order to quantify mass transfer and confirm multivalent (Mg^{2+}) uphill ion transport in the membranes. Sampling was performed only during the constant current (25 A/m²) stage every 15 min. The content of sodium ions and magnesium ions was determined by ion chromatography (Metrohm Compact IC Flex 930, Schiedam, The Netherlands).

2.4. Electrochemical measurements

A chronopotentiometric series was applied using a potentiostat

Table 1
Membrane properties of the cation exchange and anion exchange membranes used.

Membrane	Manufacturer	Characteristics	Thickness	Electrical resistance	Permselectivity
T1	Fujifilm	Magnesium permeable	115 μm	1.7 Ω cm²[a] (0.5 M NaCl)	87–91% 0.05–0.5 M NaCl[a]
CMS	Neosepta	Highly cross-linked	150 μm	1.8 Ω cm²[a]/4.7 Ω cm²[b] (0.5 M NaCl)	97% 0.05–0.5 M NaCl[a]
CSO	Selemion	One side AEM coated layer	100 μm	2.9 Ω cm²[a]	96% 0.05–0.5 M NaCl[a]
TYPE I CEM	Fujifilm	Standard membrane	115 μm	2.7 Ω cm²[a] (0.5 M NaCl)	91.9% 0.1–0.5 M NaCl[a]
TYPE I AEM	Fujifilm	Standard membrane	115 μm	1.3 Ωcm²[a] (0.5 M NaCl)	91.9% 0.1–0.5 M NaCl[a]
CMX	Neosepta	Closing membrane	155 μm	3.0 Ωcm²[a](0.5 M NaCl)	98% 0.1–0.5 M KCl[a]

[a] Given by the manufacturer.
[b] Rijnaarts et al. [10].

Table 2
Sequence of inflowing water followed during the experiments.

	Scenario 1		Scenario 2		Scenario 3		
NaCl	MgCl$_2$	NaCl	MgCl$_2$	NaCl	MgCl$_2$	NaCl	
100%	x%	100%	x%	100%	x%	100%	
Both sides	Both sides	Both sides	River water side	Both sides	Seawater side	Both sides	
1 h	1.5 h	1 h	1.5 h	1 h	1.5 h	1 h	

(Ivium Technologies, The Netherlands) every 15 min comprising of two stages. The first stage with current density steps of 2.5 A/m^2, 5.0 A/m^2, 7.5 A/m^2 and 10 A/m^2 established during 60 s to reach a constant voltage value. In between every step the current was stopped for 30 s and the OCV was measured. The sudden jump in voltage when the current is interrupted between every step reveals the stack ohmic resistance, whereas the remaining change in voltage (time-dependent) is attributed to the non-ohmic resistances. The sum of the ohmic and non-ohmic resistance equals the internal resistance of the stack (R$_{stack}$). The second stage was composed of a constant current density of 2.5 A/m^2 during 450 s. The gross power density was derived from the open circuit voltage (OCV), the stack area resistance (R$_{stack}$) and the total membrane area according to [14,15]:

$$P_{gross} = \frac{OCV^2}{4 \cdot R_{stack} \cdot N_m} \tag{1}$$

In which P$_{gross}$ is the power density (W/m^2), R$_{stack}$ is the stack area resistance (Ω m^2) and N$_m$ is the number of membranes in the stack (-). The stack area resistance was calculated from the steady state voltage during open circuit operation and during the stages with electrical current density (2.5 A/m^2, 5.0 A/m^2 and 7.5 A/m^2) using Ohm's law [4].

3. Results and discussion

The effect of MgCl$_2$ addition in the feed waters at different concentrations on a RED stack is studied by the following electrical measurements: open circuit voltage (OCV), total resistance and gross power density.

3.1. OCV

Open circuit voltage (OCV) is an appropriate measurement to visualize the effect of multivalent ions on the membrane potential. In Fig. 3, the OCV values as a function of time are presented for the four investigated CEMs and for three different concentrations of MgCl$_2$, i.e. 10%, 25% and 50% (top to bottom, respectively). Fig. 3 (top), corresponding to the experiment with 10% MgCl$_2$, shows that highest OCV values are obtained with NaCl only. In that case, OCV values follow the same order as the permselectivities of the different membranes as presented in Table 1. As soon as MgCl$_2$ is added to both or a single water type, OCV values are reduced. This effect is stronger at higher MgCl$_2$ fractions. The lower the membrane permselectivity, the higher the effect and the membrane potential drop. Also, it is clear that OCV values are most impacted when MgCl$_2$ is added to both water types (scenario 1) followed by addition to the river water (scenario 2), whereas the effect of MgCl$_2$ addition to the seawater side (scenario 3) has less impact on OCV. This can be explained because during the first scenario, Mg^{2+} ions are present at both sides and the electromotive potential over the membrane, according to the Nerst equation, is lower than when Mg^{2+} ions are only present at the river water side [6]. Switching back from MgCl$_2$ to 100% NaCl results in an almost immediate, full recovery of the original OCV values with NaCl only.

The highly cross-linked Neosepta CMS membrane is less affected by the addition of MgCl$_2$ and an almost constant voltage is maintained during the whole experiment. The high degree of cross-linking of the CMS membrane with a Na$^+$/Mg^{2+} selectivity of 34 clearly mitigates the effect of uphill and downhill transport of magnesium on the membrane potential under no current conditions [10].

The other three membranes show a clear OCV drop during all three scenarios. The magnesium permeable Fujifilm T1 membrane experiences the largest voltage drop because it is intentionally designed to allow the transport of divalent ions and a Na$^+$/Mg^{2+} selectivity of only 2, [10]. Because of its low permselectivity, the ultimate membrane potential under open circuit conditions is low. Fujifilm Type I is a standard-grade membrane without any specific strategy to allow or avoid the transport of multivalent ions. It has a comparable Na$^+$/Mg^{2+} selectivity of only 2.9 and consequently shows equal effects of the presence of MgCl$_2$ as the multivalent ion permeable membrane [10]. The Selemion CSO membrane is one-side coated with a layer of the positively charged polymer polyethylenimine (PEI) that partially rejects magnesium ions by charge repulsion [9]. Magnesium transport is minimized by this AEM coating layer and the negative effect of the presence of Mg^{2+} on the OCV is reduced.

3.2. Total resistance

In Fig. 4 the total stack resistance is plotted against time for each CEM investigated and for three different mixture concentrations, 10%, 25% and 50% MgCl$_2$.

In Fig. 4 significant differences in the total stack resistance can be observed between the different membranes. In general, Fujifilm T1, the magnesium permeable membrane, shows the lowest electrical resistance, followed by Fujifilm Type I (standard grade reference CEM), Neosepta CMS (highly cross-linked) and Selemion CSO (AEM coated). Since the AEM membranes, electrodes and electrolyte solutions are equal for all stack configurations the differences can be attributed to the type of cation exchange membrane. The stack resistance values are in accordance with the membrane resistance values reported in Table 1, except for the Neosepta CMS (highly cross-linked) membrane, which has a higher area resistance than expected. This is in accordance to other authors [16,17].

Also, it is clear that the introduction of MgCl$_2$ in the feed waters introduces an increase in stack resistance, except for the two Fujifilm membranes at 50% MgCl$_2$ in the feed waters (as will be discussed later). In general, the increase is most pronounced for the case MgCl$_2$ is introduced in both the river and the seawater compartment. This is because for this case, the absolute concentration of magnesium ions in the system is higher than when MgCl$_2$ is introduced at only one side of the membranes.

When MgCl$_2$ is only present at the river water side, uphill transport occurs and resistances show comparable behaviour as when it is introduced on both sides. Once MgCl$_2$ is introduced at the seawater side, downhill transport of magnesium ions in accordance with the concentration gradient occurs. Especially at 10% MgCl$_2$, the two Fujifilm membranes show the consequence of the lower magnesium mobility and an increase in membrane resistance is visible [10]. On the other hand, the two monovalent selective membranes, the AEM coated Selemion CSO membrane and the highly cross-linked Neosepta CMS membrane, are very well able to retain magnesium at a low magnesium concentration of only 10% and they are less affected when MgCl$_2$ is added to the seawater side.
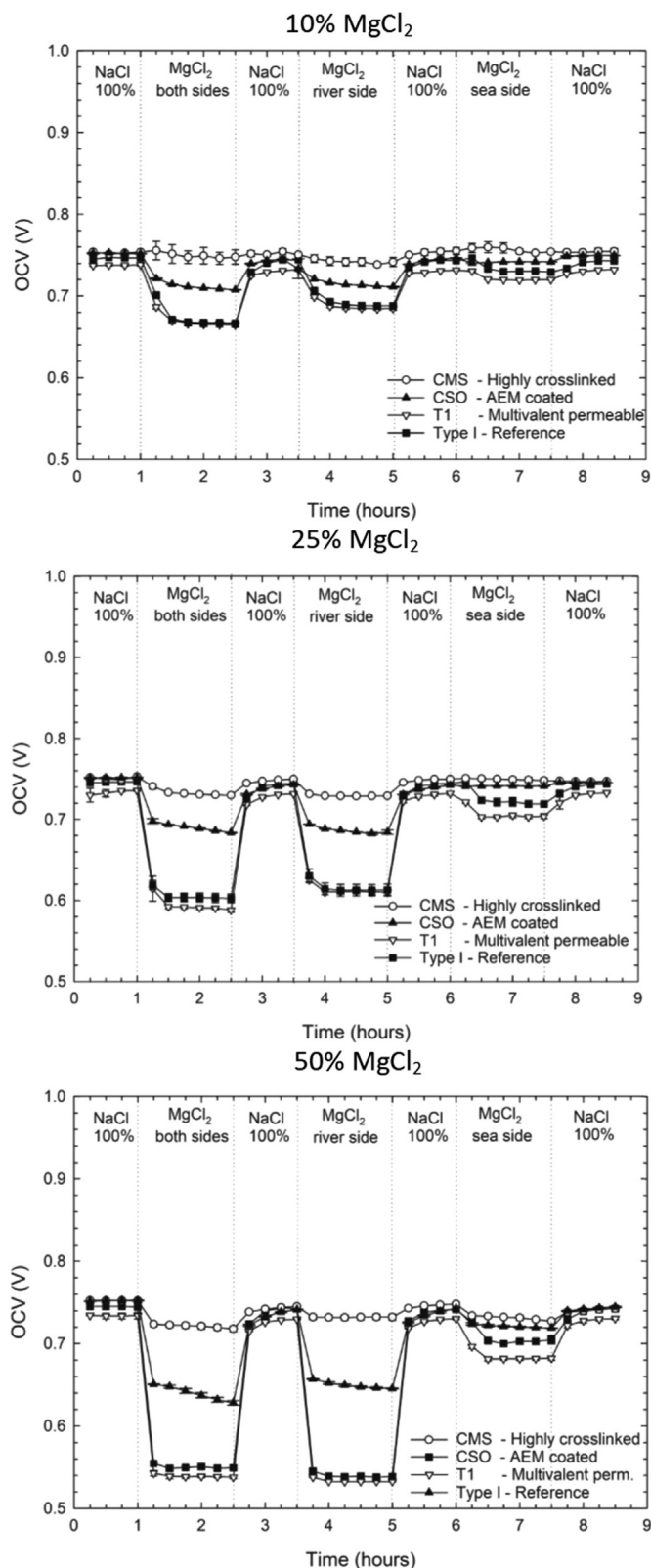
10% MgCl$_2$

10% MgCl$_2$

25% MgCl$_2$

25% MgCl$_2$

50% MgCl$_2$

50% MgCl$_2$

Fig. 3. OCV values for three different scenarios (1) MgCl$_2$ in the feed at both sides, 1–2.5 h, (2) MgCl$_2$ in the feed at the river water side only, 3.5–5 h and (3) MgCl$_2$ in the feed at the seawater side only, 6–7.5 h. Each graph represents a different concentration: (a) 10%, (b) 25% and (c) 50% MgCl$_2$ for all membranes under study: highly cross-linked Neosepta CMS, AEM coated Selemion CSO, multivalent ion permeable Fujifilm T1 and standard-grade Fujifilm Type I.
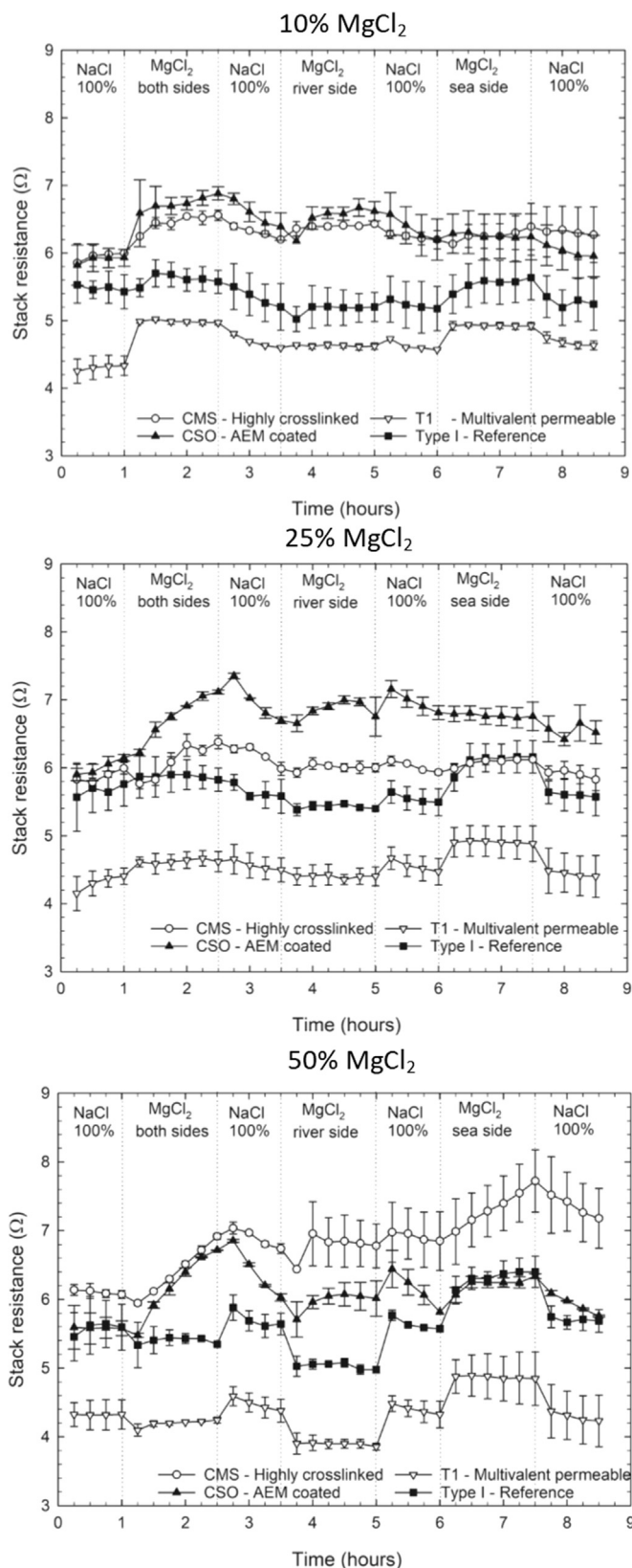
Fig. 4. Total resistance values for three different scenarios (1) MgCl$_2$ in the feed at both sides, 1–2.5 h, (2) MgCl$_2$ in the feed at the river water side only, 3.5–5 h and (3) MgCl$_2$ in the feed at the seawater side only, 6–7.5 h. Each graph represents a different concentration:, (a) 10%, (b) 25% and (c) 50% MgCl$_2$ for the membranes under study: highly cross-linked Neosepta CMS, AEM coated Selemion CSO, multivalent ion permeable Fujifilm T1 and standard-grade Fujifilm Type I.

The increase in resistance when MgCl$_2$ is introduced to the feed waters is not instantaneous, but gradual and the increase is delayed. Also the recovery of the resistance back to its original value requires some time once the feed solutions are switched back to 100% NaCl. This is especially visible for the highly cross-linked Neosepta CMS membrane, but less clear for the 'open' multivalent ion permeable Fujifilm T1 membrane. Magnesium ions are bigger and have a lower ion mobility than sodium ions [18]. As a consequence, penetration of magnesium ions into the membrane is delayed in the case of magnesium compared to sodium. This is visualized in Fig. 4 as the delayed increase in resistance. Once inside the membrane, both the lower mobility as well as the shielding of the fixed ionic charges of the membrane by the magnesium ions enhance the increase in resistance. Also, the shielding of the fixed ionic membrane charges is more effective in the case of magnesium than sodium, and thus the resistance is stronger pronounced when magnesium is present in the feed [16].

Especially when the 10%, 25% and 50% cases are compared, two different types of behaviour of the different membranes can be distinguished. The more 'open' Fujifilm membranes Type I (standard grade reference) and T1 (multivalent permeable membrane) show faster responses while switching from NaCl to MgCl$_2$ solutions and back. This is especially true at higher magnesium concentrations. Also, the relative increase in resistance is less pronounced, also especially at higher MgCl$_2$ concentrations. This is because these membranes are more open, thus less hindering the transport of magnesium in and out of the membrane. Compared to the other two types of membranes, magnesium transport through these 'open' membranes is easier. This is especially true for the magnesium permeable membrane T1. The two other membranes are especially designed to retain magnesium by a high degree of crosslinking of the membrane polymer (Neosepta CMS) or by coating an AEM layer on top of the CEM (Selemion CSO). As these two membranes are in essence designed to retain magnesium, the transport of magnesium into the membrane is significantly delayed and hindered, thus showing a more delayed but also more strong response in resistance. Once inside the membrane, it is also more difficult for magnesium ions to diffuse out of these membranes and this is visible as a delayed decrease in resistance once MgCl$_2$ is replaced for NaCl again. Moreover, especially at the 50% case during the second half of the measurement time, original NaCl resistance values are not fully recovered anymore and a shift upwards in resistance is observed for the highly cross-linked CMS membrane.

At higher concentrations of MgCl$_2$, not only the effect of magnesium on the membrane resistance is a factor that plays a role, but also the effect of the addition of additional charges (ionic species) contributes and induces an extra increase in conductivity of especially the river water compartment when adding MgCl$_2$ This effect especially is pronounced at higher MgCl$_2$ concentrations at the river water side (25% MgCl$_2$ and most dominant at 50% MgCl$_2$). At the river water side, this relative increase in conductivity is high when additional ions are added to the solution. As the river water conductivity is the dominant resistance in the stack, a little variation of this parameter influences the whole stack resistance [15,19]. So at higher MgCl$_2$ concentrations, the balance between the increase in membrane resistance and the increase in river water conductivity determines the ultimate stack resistance reported in Fig. 4.

This is most clearly visible when 50% magnesium is added and these values are compared to the 10% case. The two Fujifilm membranes allow the transport of magnesium and the relative increase in their resistances due to the presence of magnesium is limited. At the same time, when 50% MgCl$_2$ is added, the effect on the feed water (and especially the river water) conductivity is very significant and dominates over the increase in membrane resistance. This is visible as a decrease in stack resistance for these membranes in scenario 1 and 2. For the two other membranes, the membrane resistance increase dominates as these are much more sensitive to the lower magnesium ion mobility and charge shielding by magnesium ions. For the highly
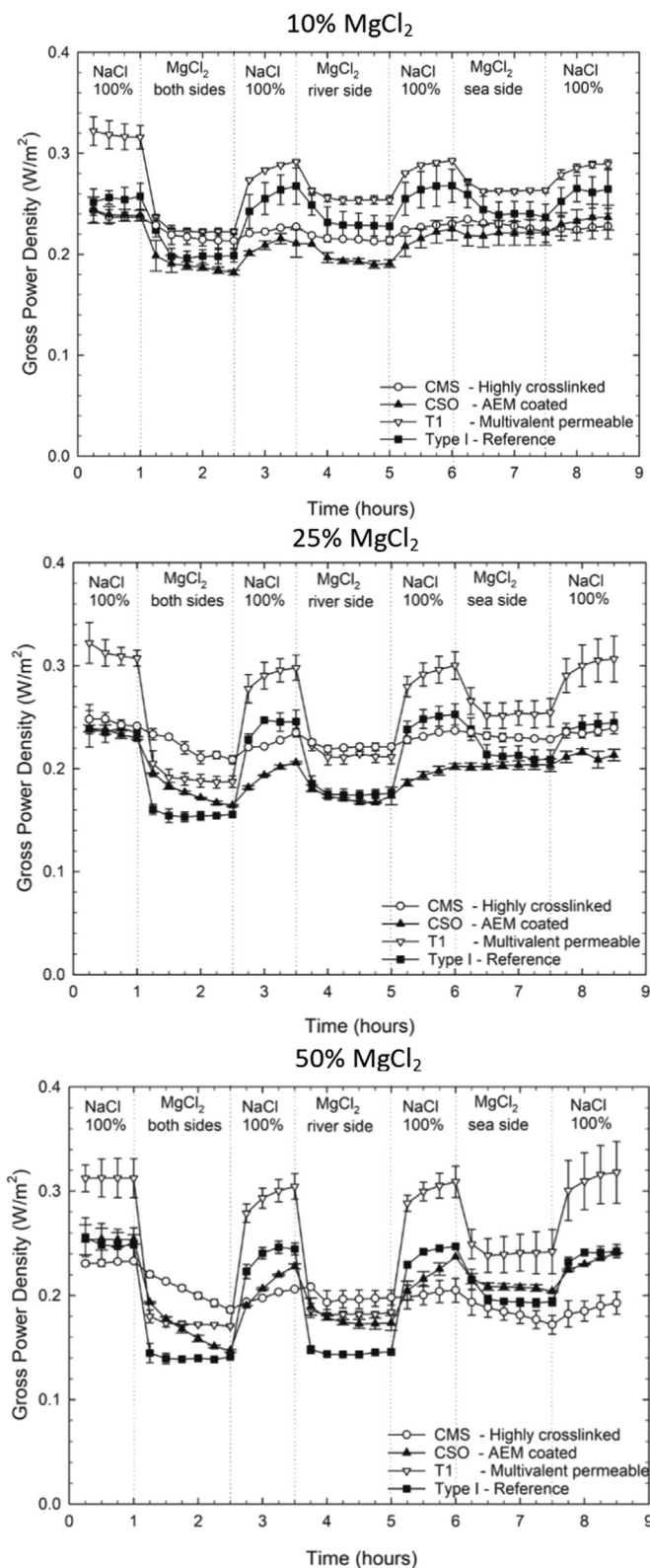

Fig. 5. Gross power density values for three different scenarios (1) MgCl$_2$ in the feed at both sides, 1–2.5 h, (2) MgCl$_2$ in the feed at the river water side only, 3.5–5 h and (3) MgCl$_2$ in the feed at the seawater side only, 6–7.5 h. Each graph represents a different concentration:, (a) 10%, (b) 25% and (c) 50% MgCl$_2$ for the membranes under study: highly cross-linked Neosepta CMS, AEM coated Selemion CSO, multivalent ion permeable Fujifilm T1 and standard-grade Fujifilm Type I.

cross-linked Neosepta CMS membrane, it was also clear that magnesium ions once inside the membrane, it is much more difficult to remove: only after feeding a highly concentrated NaCl solution (above seawater concentrations) during 1 h under 50 A/m^2 current density it was possible to reach the original membrane resistance measured in 100% NaCl.

3.3. Gross power density

In Fig. 5 the gross power density as a function of time is reported for the different CEMs and for three different concentrations of 10%, 25% and 50% MgCl$_2$. Gross power density values are the result of a combination of OCV and stack resistance.

As expected the highest gross power densities are achieved with 100% NaCl solutions as feed. The multivalent ion permeable Fujifilm T1 membrane outperforms all other membrane types under all conditions due to its low membrane resistance that more than compensates for the low OCV values of this membrane. The highest power density value for this membrane is 0.32 W/m^2, measured during the first hour of the experiment with only NaCl as feed solution.

Despite the reasonable performance at low MgCl$_2$ concentrations, the other Fujifilm membrane, the standard grade Type I reference membrane, showed the lowest performance at 25% and 50% MgCl$_2$. At these cases, the low OCV values combined with a relatively high resistance result in low gross power densities. At low MgCl$_2$ concentrations, also the reference CEM, Fujifilm Type I shows very reasonable gross power densities, especially during scenario 2 and 3. This membrane has a reasonable low resistance and a relatively high magnesium ion transfer rate. These compensate the low OCV values. However, at high MgCl$_2$ concentrations, it does not maintain its good performance and the gross power density shows a strong decrease to the lowest values measured for the different membranes. The two monovalent ion selective membranes, the highly cross-linked Neosepta CMS and the AEM coated Selemion CSO both show low performances over the full concentration and scenario range investigated. Their high resistances (especially at longer operational times and higher concentrations for the highly cross-linked membrane) dominate the OCV values.

3.4. Mass transfer balance

Both sodium and magnesium influent and effluent concentrations of the river water compartment were continuously monitored. Fig. 6 shows these concentrations during the time of the measurement for the

case with 25% MgCl$_2$ added. The difference between inlet and outlet river water concentrations represents the amount of ions transferred from river water to seawater compartment and vice versa.

Fig. 6 reflects the transport of sodium and magnesium from river water to seawater side and vice versa. In all cases, it is clear that as soon as MgCl$_2$ is introduced in the system, also influent concentrations of sodium decrease. In all cases, sodium effluent concentrations are higher than sodium influent concentrations, clearly depicting the transport of sodium ions from seawater to river water side, in accordance with the sodium concentration gradient. In Fig. 6, the effects of uphill and downhill transport are clearly depicted. In the case that MgCl$_2$ is fed to both feed water compartments, also for these two magnesium permeable membranes, magnesium concentrations in the river water effluent match those of the influent as magnesium transport occurs in both uphill and downhill direction. When MgCl$_2$ is only added to the river water side, effluent magnesium ion concentrations are clearly lower than influent concentrations, an effect being strongest for the 'open' multivalent ion permeable Fujifilm T1 membrane. This is the direct consequence of uphill transport of magnesium ions from river water to seawater compartment against the salt concentration gradient. A response time is observed between the moment magnesium is introduced in the influent and the moment a steady concentration of magnesium is reached in the effluent. This is the result of magnesium ion sorption inside the membranes. In contrast, when first a stream with a high MgCl$_2$ concentration is used, followed by a stream with a low concentration, a release of Mg^{2+} ions towards the effluent is observed.

In case MgCl$_2$ is only added to the seawater side, the opposite is observed and the magnesium concentrations in the river water effluent exceed those of the influent: the direct consequence of downhill transport.

Two different types of behaviour can be distinguished, depending on the type of membrane applied. In general the two monovalent selective membranes, the highly cross-linked Neosepta CMS membrane and the AEM coated Selemion CSO membrane are 'impermeable' for the multivalent ion magnesium. So magnesium transport is restricted. This is clearly visible in the figure above where the concentrations of magnesium in the river water effluent for both monovalent selective membranes follow the magnesium influent concentrations. Transport of charges comes fully on the account of sodium transport for the two membranes.

The two other membranes (the Fujifilm multivalent ion permeable T1 and standard grade reference Type I membranes) both allow the transport of magnesium, especially the multivalent permeable
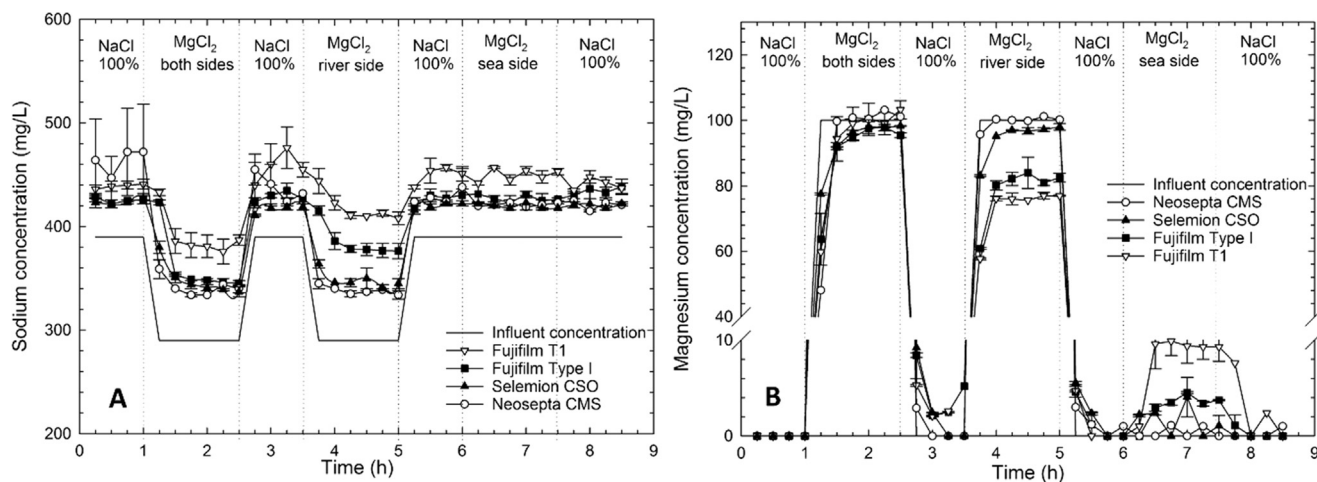

Fig. 6. (a) Sodium concentration and (b) magnesium concentration in the influent (unbroken line without symbols) and in the effluent (lines with symbols) of the river water compartment for the three different scenarios (1) MgCl$_2$ in the feed at both sides, 1–2.5 h, (2) MgCl$_2$ in the feed at the river water side, 3.5–5 h and (3) MgCl$_2$ in the feed at the seawater side, 6–7.5 h. Data for the case with 25% MgCl$_2$ added to the feed waters for all membranes under study: highly cross-linked Neosepta CMS, AEM coated Selemion CSO, multivalent ion permeable Fujifilm T1 and standard-grade Fujifilm Type I.

membrane. This is clearly visible in Fig. 6, where the effluent magnesium concentrations deviate from its influent values. As these membranes have a more 'open' structure, also sodium transport is higher for these two membranes.

During the first hour of the experiment, when 100% NaCl solution are introduced into the stacks, the highly cross-linked Neosepta CMS membrane shows the highest sodium concentration in the effluent, followed by magnesium permeable Fujifilm T1, standard-grade Fujifilm Type I and AEM coated Selemion CSO. The highly cross-linked Neosepta CMS experiment presented a strong variation during the first hour of experiment, this is due to the release of sodium ions due to regeneration process with NaCl brine after experiment at 50% $MgCl_2$ concentration.

4. Conclusions

The negative effect of multivalent ion transport against the concentration gradient, so called uphill transport, in RED can be significantly minimized when monovalent selective membranes such as the highly cross-linked Neosepta CMS membrane or the AEM coated Selemion CSO membrane are used. However, the use of such membranes directly results in a strong increase in membrane resistance due to the lower ion mobility of magnesium ions inside these membranes. As a consequence, power densities in RED are not improved. Especially at high magnesium concentrations, this effect is very strong as at higher concentrations, the membranes are no longer able to retain magnesium ions effectively.

The application of multivalent permeable membranes with a more 'open' structure that allow the free movement of both sodium and magnesium ions through the membrane. Maybe somewhat counter intuitively, such membranes (especially the Fujifilm multivalent permeable T1 membrane) have low resistance values combined with reasonable OCV values leading to high power densities under almost all magnesium concentrations.

Highest power densities are still obtained when only sodium is present and is well exceeding 0.3 W/m^2. However, when magnesium ions are present power densities in the order of 0.2–0.25 W/m^2 can still be obtained for these membranes.

The use of multivalent ion permeable membranes could be potentially more beneficial compared to monovalent selective membranes when using during long term and especially at high magnesium concentrations.

Acknowledgements

References

[1] R.E. Pattle, Production of electric power by mixing fresh and salt water in the hydroelectric pile, Nature 174 (1954) 660, http://dx.doi.org/10.1038/174660a0.

[2] R.S. Norman, Water salination: a source of energy, Science 186 (80-) (1974) 350–352.

[3] J.N. Weinstein, F.B. Leitz, Electric power from differences in salinity: the dialytic battery, Science 191 (80) (1976) 557–559.

[4] D.A. Vermaas, D. Kunteng, M. Saakes, K. Nijmeijer, Fouling in reverse electrodialysis under natural conditions, Water Res. 47 (2013) 1289–1298 ⟨http://www.sciencedirect.com/science/article/pii/S0043135412008652⟩.

[5] J.W. Post, H.V.M. Hamelers, C.J.N. Buisman, Influence of multivalent ions on power production from mixing salt and fresh water with a reverse electrodialysis system, J. Memb. Sci. 330 (2009) 65–72.

[6] D.A. Vermaas, J. Veerman, M. Saakes, K. Nijmeijer, Influence of multivalent ions on renewable energy generation in reverse electrodialysis, Energy Environ. Sci. 7 (2014) 1434–1445, http://dx.doi.org/10.1039/C3EE43501F.

[7] H. Strathmann, Ion Exchange Membrane Separation Processes, 1st ed., Elsevier, 2004.

[8] T. Badessa, V. Shaposhnik, The electrodialysis of electrolyte solutions of multicharged cations, J. Memb. Sci. 498 (2016) 86–93, http://dx.doi.org/10.1016/j.memsci.2015.09.017.

[9] E. Güler, W. van Baak, M. Saakes, K. Nijmeijer, Monovalent-ion-selective membranes for reverse electrodialysis, J. Memb. Sci. 455 (2014) 254–270, http://dx.doi.org/10.1016/j.memsci.2013.12.054.

[10] T. Rijnaarts, E. Huerta, W. van Baak, K. Nijmeijer, Effect of divalent cations on RED performance and cation exchange membrane selection to enhance power densities, Environ. Sci. Technol. 0 (n.d.) null. ⟨http://dx.doi.org/10.1021/acs.est.7b03858⟩.

[11] E.H. Martinez, Curable compositions and membranes, 2016. ⟨https://www.google.com/patents/WO2016113518A1?Cl=en⟩.

[12] T. Sata, Ion Exchange Membranes, The Royal Society of Chemistry, 2004, http://dx.doi.org/10.1039/9781847551177.

[13] T. Sata, Studies on ion exchange membranes with permselectivity for specific ions in electrodialysis, J. Memb. Sci. 93 (1994) 117–135 ⟨http://www.sciencedirect.com/science/article/pii/0376738894800014⟩.

[14] J. Veerman, J.W. Post, M. Saakes, S.J. Metz, G.J. Harmsen, Reducing power losses caused by ionic shortcut currents in reverse electrodialysis stacks by a validated model, J. Memb. Sci. 310 (2008) 418–430.

[15] D.A. Vermaas, M. Saakes, K. Nijmeijer, Double power densities from salinity gradients at reduced intermembrane distance, Environ. Sci. Technol. 45 (2011) 7089–7095.

[16] T. Rijnaarts, E. Huerta, W. Van Baak, K. Nijmeijer, RED with divalent cations: effects on performance and strategies to enhance power densities by selecting cation exchange membranes, Environ. Sci. Technol. Submitt. (2017).

[17] T. Xu, Ion exchange membranes: state of their development and perspective, J. Memb. Sci. 263 (2005) 1–29, http://dx.doi.org/10.1016/j.memsci.2005.05.002.

[18] G.M. Geise, H.J. Cassady, D.R. Paul, B.E. Logan, M.A. Hickner, Specific ion effects on membrane potential and the permselectivity of ion exchange membranes, Phys. Chem. Chem. Phys. 16 (2014) 21673–21681, http://dx.doi.org/10.1039/c4cp03076a.

[19] J. Moreno, E. Slouwerhof, D.A. Vermaas, M. Saakes, K. Nijmeijer, The breathing cell: cyclic intermembrane distance variation in reverse electrodialysis, Environ. Sci. Technol. 50 (2016), http://dx.doi.org/10.1021/acs.est.6b02668.